APPENDIX D: Nobori *et al.* (1994) *Nature* 368:753-756.

progressive renal failure, characterized rosis, interstitial fibrosis and uraemia, can suggest that the fibrosis in treated kidneys results age sustained before taxol was administered. Histolog- amination of the brain, heart, lung, liver and spleen of xol-treated polycystic mice did not reveal any gross abnormalities. Normal control mice ($n=6$) treated for 200 days with weekly doses of taxol have normal kidney histology. In addition to the survival data and renal histology, the retardation of disease progression in taxol-treated *cpk* mice was confirmed by measurements of the kidney weight, body weight and serum creatinine levels (Table 1).

Because taxol interferes specifically with microtubule functions[12], it has antimitotic properties. Inhibitors of DNA synthesis were therefore evaluated for their ability to inhibit *cpk* cyst formation *in vivo*. Weekly interperitoneal injection of 15 µl of 1.1 mg ml^{-1} methotrexate produced a reduction in growth comparable to that in mice treated with 15 µl of 10 mg ml^{-1} taxol. This sublethal weekly methotrexate treatment had no effect on the survival of polycystic *cpk* mice (Fig. 2). Sublethal doses of cytosine arabinoside (ara-C) were also ineffective (data not shown). Moreover, as doses of methotrexate and ara-C sufficient to inhibit DNA synthesis did not block lumen formation *in vitro*, the increased proliferative potential of PKD epithelia[13-16] probably does not play an important part in cyst formation but may generate cells to line expanding cysts.

Apart from their role in mitosis, microtubules contribute to and maintain cellular architecture. They also participate in membrane vesicle trafficking[17], exocytosis and endocytosis[18], and the movement of intermediate vesicles between the endoplasmic reticulum and Golgi[19,20]. During the formation of trophectoderm, microtubules play important parts in the biogenesis of epithelial polarity[21,22]. After polarity is established, specific thways deliver secreted and membrane proteins to their target embrane domains and, although these sorting processes are not well characterized, microtubules are clearly involved[23,24]. Our data implicate the microtubule network in the genesis of PKD cysts both *in vitro* and *in vivo*. It remains to be determined whether altered tubulins or altered microtubule-associated proteins are primary lesions in *cpk* mice or other forms of PKD. It is feasible that aberrations of cellular functions mediated by microtubules may lead to the apical mislocation of Na^+, K^+-ATPase and epidermal growth factor receptors in both human[25] and murine PKD[26]. Finally, the ability of taxol to prevent the uraemic death in a mouse model for PKD suggests that taxol or its analogues may be useful in the treatment of human polycystic kidney diseases. □

Received 7 October 1993; accepted 4 February 1994.

1. Russell, E. S. & McFarland, E. *Mouse Newsletter* **56**, 40 (1977).
2. Preminger, G. M., Koch, W. E., Fried, F. A., McFarland, E. & Murphy, E. M. *J. J. Urol.* **127**, 556–560 (1982).
3. Avner, E. D. *et al. Pediat. Nephrol.* **1**, 587–596 (1987).
4. Wilson, P. D., Schrier, R. W., Breckon, R. D. & Gabow, P. A. *Kidney Int.* **30**, 371–378 (1986).
5. Yang, A. H., Gould, K. J. & Oberley, T. D. *In Vitro Cell Dev. Biol.* **23**, 34–46 (1987).
6. Carone, F. A., Nakamura, S., Schumacher, B. S., Punyarit, P. & Bauer, K. D. *Kidney Int.* **35**, 1351–1357 (1989).
7. Valentich, J. D., Tchao, R. & Leighton, J. *J. Cell Physiol.* **100**, 291–304 (1979).
8. Mangoo, K. R. *et al. FASEB J.* **3**, 2629–2632 (1989).
9. Neufeld, T. K. *et al.* **41**, 1222–1236 (1992).
10. Fleming, T. P. & Johnson, M. H. *A. Rev. cell. Biol.* **4**, 459–485 (1988).
11. Brenner, B. M. *Kidney Int.* **23**, 647–655 (1983).
12. Schiff, P. & Horwitz, S. *Proc. natn. Acad. Sci. U.S.A.* **77**, 1561–1565 (1980).
13. Gattone, V. H. *et al. Lab. Invest.* **59**, 231–238 (1988).
14. Cowley, B. D. J., Smardo, F. L. J., Grantham, J. J. & Calvet, J. P. *Proc. natn. Acad. Sci. U.S.A.* **84**, 8394–8398 (1987).
15. Avner, E. D., Sweeney, W. E. J., YOung, M. C. & Ellis, D. *Pediat. Nephrol.* **2**, 210–218 (1988).
16. Cowley, B., Chadwick, L., Grantham, J. & Calvert, J. *J. Am. Soc. Neph.* **1**, 1048–1053 (1991).
17. Kelly, R. *Cell* **60**, 5–7 (1990).
18. Rogalski, A. A., Bergmann, J. E. & Singer, S. J. *J. Cell Biol.* **99**, 1101–1109 (1984).
19. Thyberg, J. & Moskalewski, S. *Exp! Cell Res.* **159**, 1–16 (1985).
20. Lippincott-Schwartz, J. *et al. Cell* **60**, 821–836 (1990).
21. Bloom, T. *Development* **108**, 159–171 (1989).
22. Maro, R., Gueth-Hallonet, C. J. A. & Antony, C. *Development* Vol. 1, suppl. 1. 17–25 (1991).
23. Parczyk, K., Haase, W. & Kondor-Koch, C. *J. biol. Chem.* **264**, 16837–16846 (1989).
24. De Almeida, J. B. & Stow, J. L. *Am. J. Physiol.* **260**, C691–C700 (1991).
25. Wilson, P. D. *et al. Am. J. Physiol* **260**, F420–F430 (1991).
26. Avner, E., Sweeney, W. & Nelson, W. *Proc. natn. Acad. Sci. U.S.A.* **89**, 7447–7451 (1992).
27. Slot, C. *Scand. J. Clin. Lab. Invest.* **17**, 381–387 (1965).

ACKNOWLEDGEMENTS. This work is supported by NIH grants and A.S.W. is a National Kidney Research Fund Senior Fellow. Normal and polycystic human kidneys are obtained from the International Institute for the Advance of Medicine (Exton, Pennsylvania), the National Disease Research Interchange (Philadelphia) and the Polycystic Kidney Research Foundation (Kansas City).

Deletions of the cyclin-dependent kinase-4 inhibitor gene in multiple human cancers

Tsutomu Nobori*, Kaoru Miura*, David J. Wu*, Augusto Lois*, Kenji Takabayashi† & Dennis A. Carson*

* Department of Medicine, University of California, San Diego, 9500 Gilman Drive, La Jolla, California 92093-0663, USA
† CIBA–GEIGY Pharmaceuticals Division, CH-4002 Basel, Switzerland

CYTOGENETIC abnormalities of chromosome 9p21 are characteristic of malignant melanomas[1,2], gliomas[3], lung cancers[4] and leukaemias[5]. From a panel of 46 human malignant cell lines, we localized by positional cloning the most frequently deleted region on 9p21. Sequence analysis of the isolated fragment reveals two open reading frames identical to the recently described complementary DNA for the inhibitor of cyclin-dependent kinase 4 (CDK4)[6]. Polymerase chain reaction and Southern blot analysis confirmed the frequent deletion or rearrangement of the CDK4-inhibitor gene in melanomas, gliomas, lung cancers and leukaemias, and the absence of detectable gene transcripts. One carcinoma had a deletion entirely within the CDK4-inhibitor gene. The CDK4-inhibitor gene from a patient with dysplastic nevus syndrome had a germline nonsense mutation. The CDK4 inhibitor is thought to be a physiological suppressor of proliferation. Cells unable to produce the inhibitor may be prone to neoplastic transformation.

Many malignant cell lines with chromosome 9p21 deletions either lack the enzyme methylthioadenosine phosphorylase (MTAP), or have hemizygous or homozygous deletions of the interferon-α (*IFN-α*) gene cluster[5,7,8]. The T98G glioma cell line has a small 9p deletion centromeric to the *IFN-α* locus, but has normal methylthioadenosine phosphorylase activity[5]. These results suggested that the putative tumour-suppressor gene on chromosome 9p resided between the *MTAP* and *IFN-α* loci.

MTAP cDNA was isolated and used to probe a human placenta λ-phage library. A 2-kilobase (kb) *Hin*dIII fragment (clone 7-2) contained the 3′ end of the *MTAP* gene by sequence analysis. Chromosome walking was performed, starting with the 3′ end of *MTAP*. Several screening cycles of P1 phage[9], and subsequent λ-phage libraries led to the isolation of clones encompassing the deleted region in T98G. Restriction fragments of these phage were subcloned, partially sequenced, and mapped by Southern blotting and pulsed-field gel electrophoresis. Figure 1 shows the map of human chromosome 9p21 between the *MTAP* and interferon-β (*IFN-β*) gene loci, focusing on the deleted segment in T98G.

The polymerase chain reaction (PCR) was used to determine the frequency of deletion of several-tagged sites (STS) from chromosome 9p in 46 different human malignant cell lines (Table 1). Depending on the cell type, either STS *54F* or STS *5BS* was deleted most frequently. These results focused our attention on the 50-kb region between STS *54F* and STS *5BS*.

Eight malignant cell lines with breakpoints between *54F* and *5BS* were then analysed by STS-PCR, with new probes from the intervening region. The deletion maps are shown at the

TABLE 1 Homozygous loss of chromosome 9p loci in human cancer cells

Cell line (number)		Frequency of negative STS-PCR (%)									
		MTAP	*3.21*	*2F*	*54F*	*CDK4I*	*5BS*	*71F*	*3.3B*	*IFN-α8*	*IFN-β*
Melanoma	(13)	30.8	38.5	53.8	53.8	61.5	61.5	61.5	15.4	7.7	0
Glioma	(8)	62.5	75.0	87.5	87.5	87.5	75.0	75.0	62.5	62.5	25.0
Lung cancer	(11)	27.3	27.3	27.3	27.3	36.4	36.4	36.4	9.1	9.1	0
Leukaemia	(14)	50.0	50.0	64.3	64.3	64.3	57.1	57.1	28.6	28.6	21.4

Homozygous deletion of these loci was detected by STS-PCR. PCR, except for *CDK4I* and *CDK4I3'*, was carried out in a total volume of 20 μl, containing 0.1 μg of genomic DNA, 1 × PCR buffer (10 mM Tris-HCl, pH 8.3, 50 mM KCl, 1.5 mM $MgCl_2$, 0.01% gelatin), 200 μM of each dNTP, 20 ng each of sense and antisense primers, and 0.5 units of *Taq* DNA polymerase. Thirty cycles were performed, each cycle consisting of denaturation (94 °C, 1 min), annealing (50 °C or 55°C, 1 min), and extension (72 °C, 1 min). 10-μl aliquots were resolved on 2% agarose gels. The locations of the STS-PCR sites are shown in Fig. 1a. CDK4I-PCR was performed as described for Fig. 2.

bottom of Fig. 1. A 19-kb λ-phage clone (10B1) identified the most frequently deleted site. We concluded that the 10B1 phage should contain part of the putative tumour-suppressor gene.

The sequence of a plasmid subclone (10B1-10) from 10B1 contained a 306-base-pair (bp) open reading frame with sequence identity to the 3' region of the recently described cDNA for the human cyclin-dependent kinase-4 (CDK4) inhibitor, apart from the last 15 bp[8] (Fig. 2a). The 3' end of the coding region, and the 3' non-coding region, was located 2.6 kb towards *MTAP*. The 5' end of the gene was telomeric to the deleted region in T98G (Fig. 1). We rescreened the 46 malignant cell lines with STS-PCR primers, corresponding to the isolated fragment of the CDK4-inhibitor gene, designated *CDK4I* in Table 1. Sixty-one per cent of melanomas, 87% of gliomas, 36% of non-small-cell lung cancers, and 64% of leukaemias have homozygous deletions of the *CDK4I* gene fragment. Melanoma cell line WM266-4 has only the 5' end of the CDK4-inhibitor gene deleted. It was positive for STS *CDK4I*, negative for STS *5BS*, and produced an abnormal 7.0-kb band after *Eco*RI digestion, electrophoresis and hybridization to a probe from the 5' region of the CDK4-inhibitor gene (Fig. 2c). On the other hand, melanoma cell line SK-MEL-31 has only the 3' end of the CDK4-inhibitor gene deleted. It was negative for STS *CD4KI* (Fig. 2b), but produced a normal 4.0-kb band, indistinguishable from

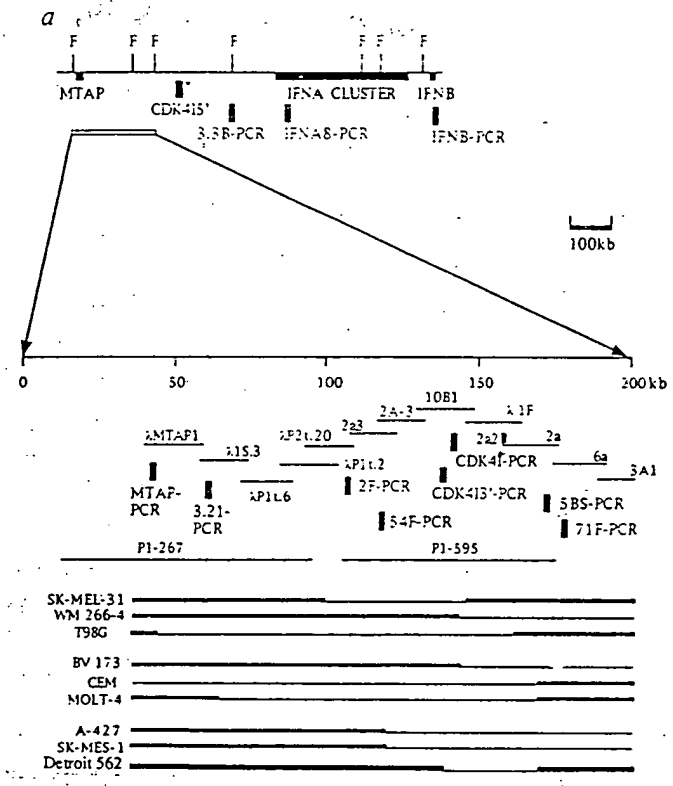

FIG. 1 Physical map of chromosome 9p21 between the *MTAP* and *IFN-β* gene loci. *a*, The P1 phage clones and λ-phage clones are indicated by thin lines. The sequence-tagged sites (STSs) used for PCR are shown as cross-hatched bars. The *CDK4I* and *CDK4I3'* sequences come from phage 10B1 and are separated by a 2.6-kb intron. These 11 STS-PCR assays localized the approximate breakpoints in the nine malignant cell lines with the most informative deletions. SK-MEL-31 and WM 266-4 are melanomas; T98G is a glioma; BV173, CEM, and MOLT-4 are leukaemias; A-427 and SK-MES-1 are non-small-cell lung cancers; Detroit 562 is a pharyngeal carcinoma. Homozygous deletions are indicated by thin horizontal lines. Asterisk indicates that the location of *CDK4I5'* in the 190-kb *Sfi*I fragment is not precise. F, *Sfi*I. *b*, STS-PCR analysis. All STS-PCR amplified fragments of the expected size in J640-51 cells containing a single human chromosome 9 on a Chinese hamster background (data not shown). Lanes: 1, human placenta; 2, SK-MEL-31; 3, WM 266-4; 4, T98G; 5, BV173; 6, CEM; 7, MOLT-4; 8, A-427; 9, SK-MES-1; 10, no template DNA; 11, DNA markers.

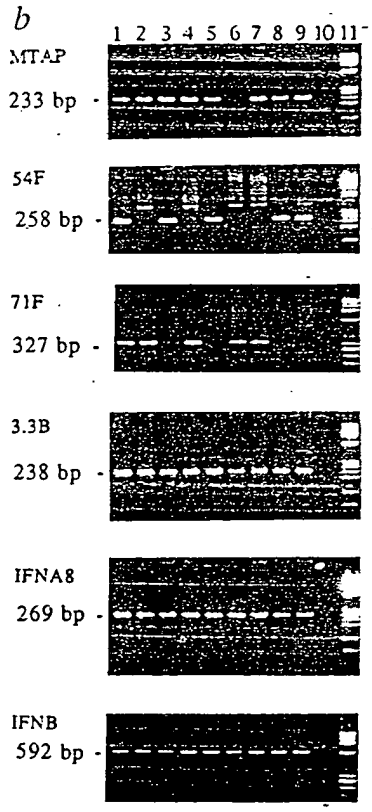

METHODS. *a*, The λMTAP1 clone was obtained by screening a human placenta λFIX II genomic library (Stratagene) with MTAP cDNA. A 2-kb *Hin*dIII fragment containing the 3' end of the *MTAP* gene was used for chromosome walking in human P1 phage (Genome Systems), λ-phage (Stratagene), and chromosome-9-specific charon-40 phage (LL09NL02, ATCC) libraries. Clones encompassing the 190-kb region were isolated, subcloned, partially sequenced, and mapped by southern and pulsed field-gel blotting. *b*, STS-PCR was developed on the basis of the partial sequences of the subclones. PCR amplification was done under conditions described in Table 1. PCR products were resolved on a 2% agarose gel.

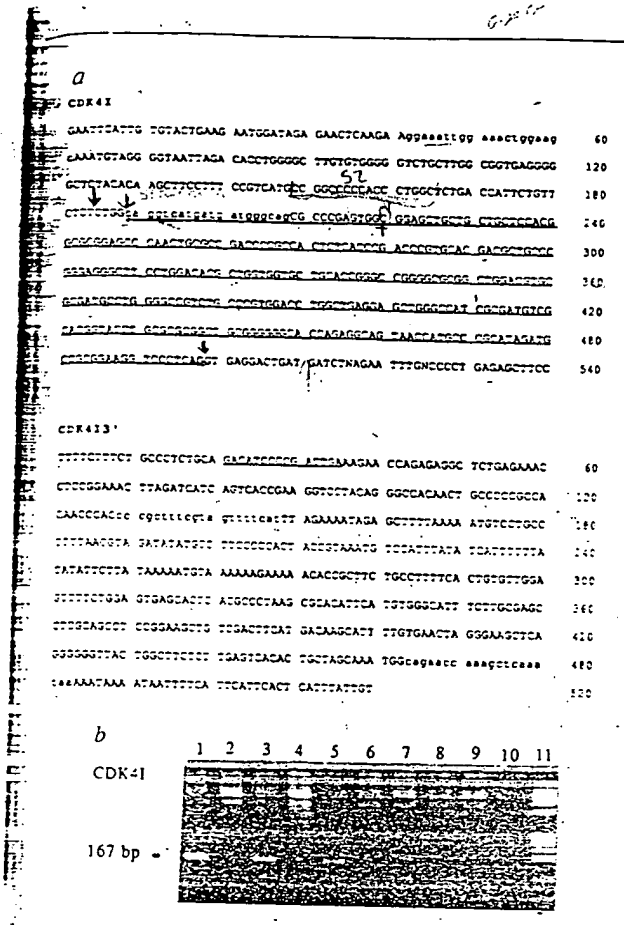

FIG. 2 Absence or rearrangement of the CDK4-inhibitor gene in malignant cell lines. *a*, Partial sequence of the genomic CDK4-inhibitor gene. The genomic sequence designated *CDK4I* has a 306-bp open reading frame with complete sequence identity to CDK4-inhibitor cDNA, from nucleotides 192 to 497 (underlined). The CDK4I3' sequence has a short open reading frame (underlined) corresponding to the last 15 bp of the coding region, with a stop codon and the 3' non-coding sequence, except for two nucleotides (T at 197 and A at 493). *b*, PCR analysis of malignant cell lines. Primers for *CDK4I*, shown as lower-case letters in *a*, were used to amplify an expected 167-bp product in human placenta (lane 1) SK-MEL-31 (lane 2), WM 266-4 (lane 3), T98G (lane 4), BV173 (lane 5), CEM (lane 6), MOLT-4 (lane 7), A-427 (lane 8), and SK-MES-1 (lane 9). Lane 10 has no template DNA. Lane 11 shows DNA markers. *c*, Southern blot analysis of melanoma cell lines hybridized to probes 2a2 and CDK4I5'. In *Sfi*I-digested pulsed-field blots, 2a2 hybridized to a 54-kb fragment. CDK4I5' hybridized to a 190-kb fragment which was also detected with the 3.3B probe in the same blot (data not shown). Lanes: 1, human placenta; 2, Hs294T; 3, HT144; 4, RPMI7951; 5, SK-MEL-1; 6, SK-MEL-2; 7, SK-MEL-3; 8, SK-MEL-28; 9, SK-MEL-31; 10, WM 266-4.

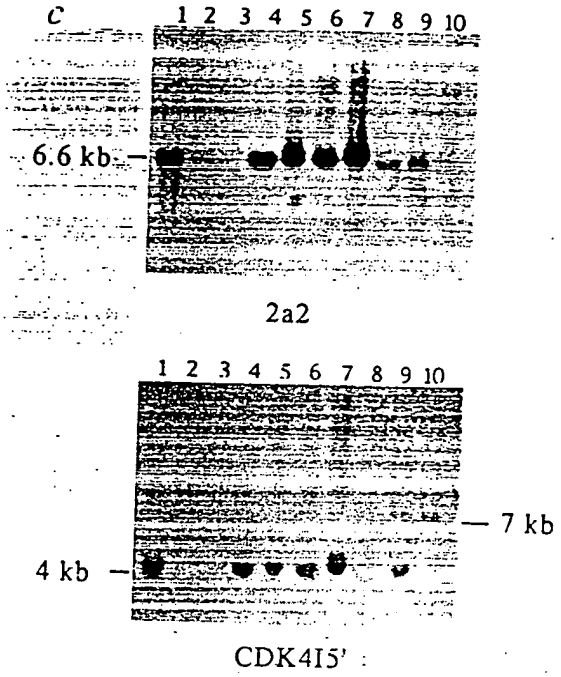

METHODS. *a*, Phage DNA of clone 10B1 was digested with *Eco*RI and subcloned into *Eco*RI-cut pBluescriptII SK(+) (Stratagene). Subclones were subjected to automated DNA sequencing. The 4.2-kb subclone 10B1-10 contained both the *CDK4I* and the *CDK4I3'* sequences. *b*, PCR amplification was carried out as described in Table 1 legend except that 35 cycles were performed and annealing was at 64 °C and extension at 72° C. PCR was followed by gel electrophoresis. *c*, DNAs from human placenta and melanoma cell lines were digested with *Eco*RI, resolved on a 0.8% agarose gel, and transferred to nylon membranes. 2a2 is a 1.3-kb *Eco*RI–*Xho*I fragment of phage clone 2a. CDK4I5' is a 139-bp product generated by RT-PCR. cDNA from cell line H661 was amplified by PCR using a sense primer (5'-AATTCGGCACGAGGCAGCAT-3') and an antisense primer (5'-TTATTTGAGCTTTGGTTCTG-3'). PCR products were subcloned and sequenced. Clone p7-4 contained the 5' sequence of CDK4-inhibitor cDNA. A 139-bp product was amplified from clone p7-4 with a sense primer and a new antisense primer (5'-TCGGCCTCCGACCGTAACTA-3') and used for Southern blotting. Blots were hybridized at 65 °C overnight, washed at 65 °C in 0.1 × SSC containing 0.1% SDS, and exposed to X-ray film. After stripping off radioactivity, the same membrane was rehybridized with probe 2a2.

FIG. 3 Reverse transcriptase-PCR amplification of CDK4-inhibitor mRNA from human malignant cells lines. The glyceraldehyde 3-phosphate dehydrogenase gene (G3PDH) mRNA served as a control. WI-L2 in lane 1 is a normal lymphoblastoid cell line. U937 in lane 2 is a leukaemia cell line. T98G in lane 3 is a glioma cell line. H661 in lane 4, A-549 in lane 5, and SK-MES-1 in lane 6 are non-small-cell lung cancer cell lines. Lane M shows DNA markers. STS-PCR analysis confirmed the presence of STS CDK4I in WI-L2, U937, and H661 (data not shown). T98G and SK-MES-1 have the 9p21 deletions shown in Fig. 1a. The deletion in cell line A-549 spans STS *MTAP* to *71F* (data not shown). CDK4-inhibitor mRNA was not detected in cell lines with 9p21 deletions that included the CDK4-inhibitor gene.

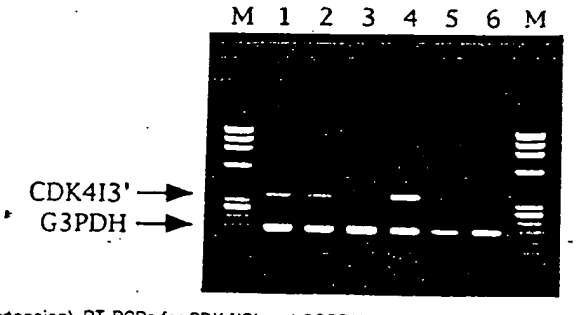

METHODS. mRNA was purified with a FastTrack kit (Invitrogen) and was treated with RNase-free DNase I (Pharmacia) using human placenta DNA as a control to ensure complete digestion by DNase I. After first-strand cDNA synthesis with a Stratascript RT-PCR kit (Stratagene), cDNA was amplified with the CDK4I3' primers shown in lower-case in Fig. 2a (58 °C annealing and 70 °C extension). Primers for the G3PDH gene (5'-TGGTATCGTGGAAGGACTCATGAC-3' and 5'-ATGCCAGTGAGCTTCCCGT-TCAGC-3') amplified a 190-bp product (55 °C annealing and 72 °C extension). RT-PCRs for CDK4I3' and G3PDH were done separately and resolved on a 2% agarose gel by loading onto the same lanes. As no product was amplified in DNase I-treated human placenta DNA with the CDK4I3' primers, the 355-bp RT–PCR product seen in lanes 1, 2 and 4 was derived from cDNA. Sequence analysis of the RT-PCR products confirmed the CDK4I cDNA sequence.

placental DNA, after *Eco*RI digestion, and hybridization to the 5'-region probe from the CDK4-inhibitor gene. The most informative cell line was Detroit 562 (a pharyngeal carcinoma) which has a 29-kb deletion within the CDK4-inhibitor gene (Fig. 1). It was positive for STS *CDK4I3'*, negative for STS *CDK4I*, but positive for STS *5BS* and STS *7IF*. The last two STSs are centromeric to the 5' end of the CDK4-inhibitor gene.

Reverse transcriptase-polymerase chain reaction (RT-PCR) assays revealed CDK4-inhibitor gene transcripts in normal cells, but not in cancers with established deletions of the CDK4-inhibitor gene (Fig. 3). Collectively, these results indicate that human cells contain a single CDK4-inhibitor gene, which is homozygously deleted or rearranged in the majority of melanomas, gliomas and leukaemias, and in almost one-third of non-small-cell lung cancers.

The complexes formed by CDK4 and the D-type cyclins control passage through the G1 phase of the cell cycle[6]. The inhibitor of CDK4 is a protein of relative molecular mass 16K which binds to and inhibits the catalytic activity of the CDK4/cyclin D enzymes. Because it is a negative regulator of cell-cycle progression, the inhibitor of CDK4 may be inactivated during cancer development[10]. The product of the p53 gene also inhibits growth by stimulating the production of a CDK-inhibitory protein[11,12].

About 10% of melanomas are familial[2]. [illegible] pinpointed the locus for familial melanoma [illegible] 9p21 that is deleted in sporadic melanomas[13]. [illegible] of the CDK4I coding region of a lymph[illegible] (GM06921) derived from a patient with dy[illegible] drome (familial melanoma) showed a C to T [illegible] tion 166 of the mRNA[6] resulting in a nonsc[illegible] the CDK4 inhibitor is a strong candidate [illegible] susceptibility gene.

Received 25 February; accepted 28 March 1994.

1. Fountain, J. E. *et al. Proc. natn. Acad. Sci. U.S.A.* **89**, 10557–[illegible]
2. Petty, E. M. *et al. Am. J. hum. Genet.* **53**, 96–104 (1993).
3. Olopade, O. I. *et al. Cancer Res.* **52**, 2523–2529 (1992).
4. Olopade, O. I. *et al. Cancer Res.* **53**, 2410–2415 (1993).
5. Olopade, O. I. *et al. Genomics* **14**, 437–443 (1992).
6. Serrano, M., Hannon, G. J. & Beach, D. *Nature* **366**, 704–707 [illegible]
7. Nobori, T. *et al. Cancer Res.* **51**, 3193–3197 (1991).
8. Nobori, T. *et al. Cancer Res.* **53**, 1058–10101 (1993).
9. Pierce, J. C. & Sternberg, N. L. *Meth. Enzym.* **216**, 549–574 [illegible]
10. Marx, J. *Science* **263**, 319–321 (1994).
11. Harper, J. W., Adami, G. R., Wei, N., Keyomarsi, K. & Elledge, S. J. [illegible]
12. Xiong, Y. *et al. Nature* **366**, 701–704 (1993).
13. Cannon-Albright, L. A. *et al. Science* **258**, 1148–1152 (1992).

ACKNOWLEDGEMENTS. We thank L. Orvis, A. Larson, P. Tran and [illegible] assistance; C. Jones for J640-51 hybrid cells, and L. Bibbs for [illegible] Supported by grants from the NIH, the American Cancer Society, [illegible] Tobacco Related Diseases Research Program, and the CIBA–GEIGY [illegible]

Pancreatic islet cell toxicity of amylin associated with type-2 diabetes mellitus

Alfredo Lorenzo*, Bronwyn Razzaboni*, Gordon C. Weir† & Bruce A. Yankner*‡

* Department of Neurology, Harvard Medical School and The Children's Hospital, Enders 260, 300 Longwood Avenue, Boston, Massachusetts 02115, USA
† Joslin Diabetes Center and Harvard Medical School, Boston, Massachusetts 02215, USA

THE 37-amino-acid polypeptide amylin is the principal constituent of the amyloid deposits that form in the islets of Langerhans in patients with type-2 diabetes mellitus[1–5], but its role in the pathogenesis of this disease is unresolved[6–8]. In view of the fact that the β-amyloid protein that forms fibrils in Alzheimer's disease is toxic to neurons[9,10], we have investigated whether amylin fibrils could be toxic to pancreatic islet cells. We show here that human amylin is toxic to insulin-producing β-cells of the adult pancreas of rats and humans. This toxicity is mediated by the fibrillar form of the amylin peptide and requires direct contact of the fibrils with the cell surface. The mechanism of cell death involves RNA and protein synthesis and is characterized by plasma membrane blebbing, chromatin condensation and DNA fragmentation, indicating that amylin induces islet cell apoptosis. These findings indicate that amylin fibril formation in the pancreas may cause islet cell dysfunction and death in type-2 diabetes mellitus.

Islet cell cultures were established from adult rat pancreas and cell viability was assessed by a double-fluorescence assay. Exposure to human amylin resulted in substantial rat islet cell death after 24 h (Fig. 1*a*, *b*). Immunocytochemical analysis showed that human amylin caused the degeneration of 97 ± 1% (mean ± s.e.m., $n = 15$; $P < 0.001$ by ANOVA) of insulin-producing islet cells (Fig. 1*c*, *d*). Amylin was also toxic to human islet cells isolated from the pancreas of a 39-year-old woman. Incubation of dissociated human islets with human amylin resulted in the degeneration of 91 ± 2% ($n = 15$; $P < 0.001$) of insulin-producing islet cells (Fig. 1*e*, *f*). Incubation of non-disso-

FIG. 1 Toxicity of human amylin [illegible] cells. *a*, Control rat islet cells treated with [illegible] with calcein–AM and propidium iodide. Epifluorescence shows viable cells which convert the calcein–AM [illegible] fluorescent product. *b*, Rat islet cells after treatment with 20 [illegible] amylin for 24 h. There are many dead cells which show red [illegible] due to nuclear uptake of propidium iodide and few viable [illegible] show green calcein fluorescence. Insulin immunocytochem[illegible] trol (*c*) and human amylin-treated rat islet (*d*) cells; *e*, [illegible] human amylin-treated human islet cells; *g*, control, and [illegible] amylin-treated, non-dissociated human islets. Note the [illegible] insulin-positive islet cells after exposure to human amyl[illegible] Scale bars: *a*, 40 μm; *c*, *e* and *g*, 20 μm.

METHODS. Islet cell cultures were maintained for 3–4 [illegible] viability) and then treated with vehicle or 20 μM human amyl[illegible] Pancreatic islets were isolated by perfusion of the rat pan[illegible] adult male Sprague-Dawley rats weighing 180–20[illegible] collagenase[27]. Human islets were isolated from the pancr[illegible] year-old woman as described[28]. Isolated islets were [illegible] incubation in trypsin–EDTA for 10 min at 37 °C and repetitive [illegible] with a Pasteur pipette. Dissociated islet cells or non-dissoci[illegible] were cultured in 16-mm tissue-culture wells on glass cover[illegible] with Matrigel (Collaborative Biomedical Products) in 300 [illegible] of RPMI 1640 medium supplemented with 10% fetal bov[illegible] 100 U ml^{-1} penicillin and 100 μg ml^{-1} streptomycin. Lyophi[illegible] tides were dissolved in water to 346 μM and immediately [illegible] culture medium at the indicated concentration. An equal [illegible] sterile water was added to control cultures. Cell viability was [illegible] by the calcein–AM/propidium iodide double-staining method (Molecular Probes)[29]. Culture medium was removed after treatment and cells incubated with 1 μM calcein–AM and 10 μg ml^{-1} propidium iodide in phosphate-buffered saline (PBS) for 10 min at 37 °C. Viable cells convert calcein–AM to calcein, producing uniform green fluorescence. Dead cells take up propidium iodide into the nucleus, resulting in a red fluorescence. Green and red fluorescence were simultaneously visualized using a Nikon transmission microscope equipped with a 530-nm pass filter. For immunocytochemistry, cultures were fixed in 4% paraformaldehyde, 0.12 M sucrose in PBS, pre-incubated with 5% normal goat serum and stained with a polyclonal primary antibody against human insulin using the DAKO PAP kit. Fixed sections of pancreatic tissue were used as a positive control. The viability of insulin-positive cells was determined by propidium iodide staining and scored as described in Table 1. HPLC-purified human, rat and cat amylin (full-length 37-amino-acid peptides) were obtained from Bachem California and Peninsula Laboratories. Human amylin from both sources gave the same results. Peptides were analysed by laser desorption mass spectroscopy. Molecular values: human 3,903 ± 2 (mean ± s.e.m., $n = 8$; predicted M_r 3,904); cat 3,910 ± 1 ($n = 3$; predicted M_r 3,909); rat 3,919 ± 2 ($n = 4$; predicted M_r 3,921)).

‡ To whom correspondence should be addressed.